SUPPLEMENTAL MATERIAL

Gosselin-Badaroudine et al., http://www.jgp.org/cgi/content/full/jgp.201611614/DC1

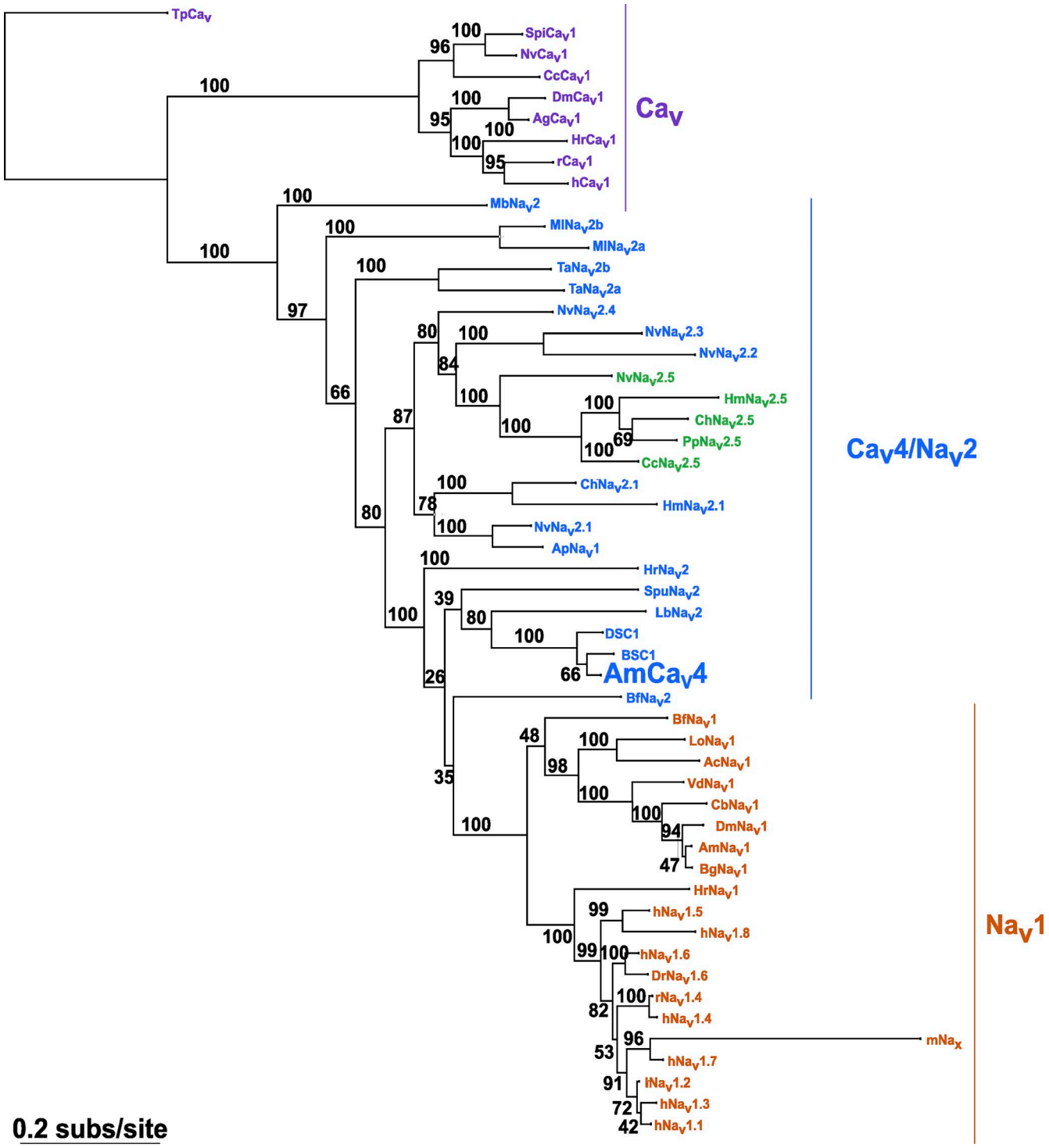


Figure S1. **AmCaV4 belongs to the CaV4/NaV2 ion channel family.** A maximum-likelihood tree was generated using the PHYLIP package on an alignment comprising both sodium Nav channels identified in the honeybee genome and the GenBank sequences used by Gur Barzilai et al. (2012). The bootstrap support (out of 100) is displayed on the branches. Cav channels are shown in purple. Nav1 channels are in orange, and channels previously identified as Nav2 channels are in blue, with the exception of channels that feature the DKEA selectivity sequence, which are displayed in green.

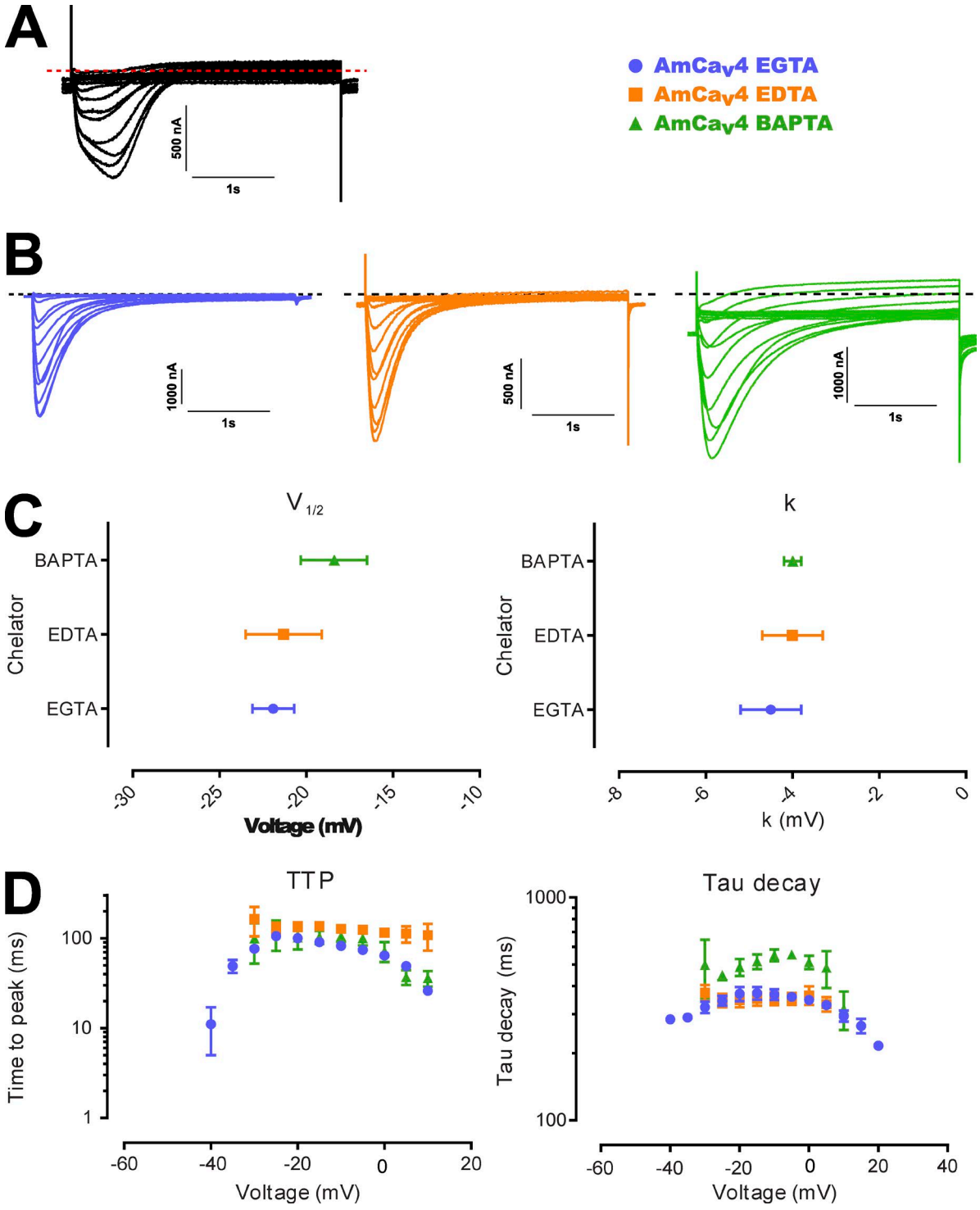


Figure S2. **The use of chelating solutions abolishes contamination of the $Ca^{2+}$ current by endogenous $Ca^{2+}$-activated chloride currents.** (A) Oocytes expressing $AmCa_V4$ displayed a robust inward current characterized by two sets of slow kinetics as a response to depolarizing steps from −65 to 25 mV. (B) Currents recorded when oocytes were injected with a chelating solution before experiment displayed only one set of kinetics. (C) The fit parameters for the voltage dependence of activation were not statistically different when EDTA or BAPTA were used instead of EGTA in the chelating solution. (D) Time constants for current onset and decay were slightly different when EDTA or BAPTA were used instead of EGTA in the chelating solution. The oocytes injected with EGTA chelating solution displayed the fastest kinetics and lowest leak. Error bars represent SEM.

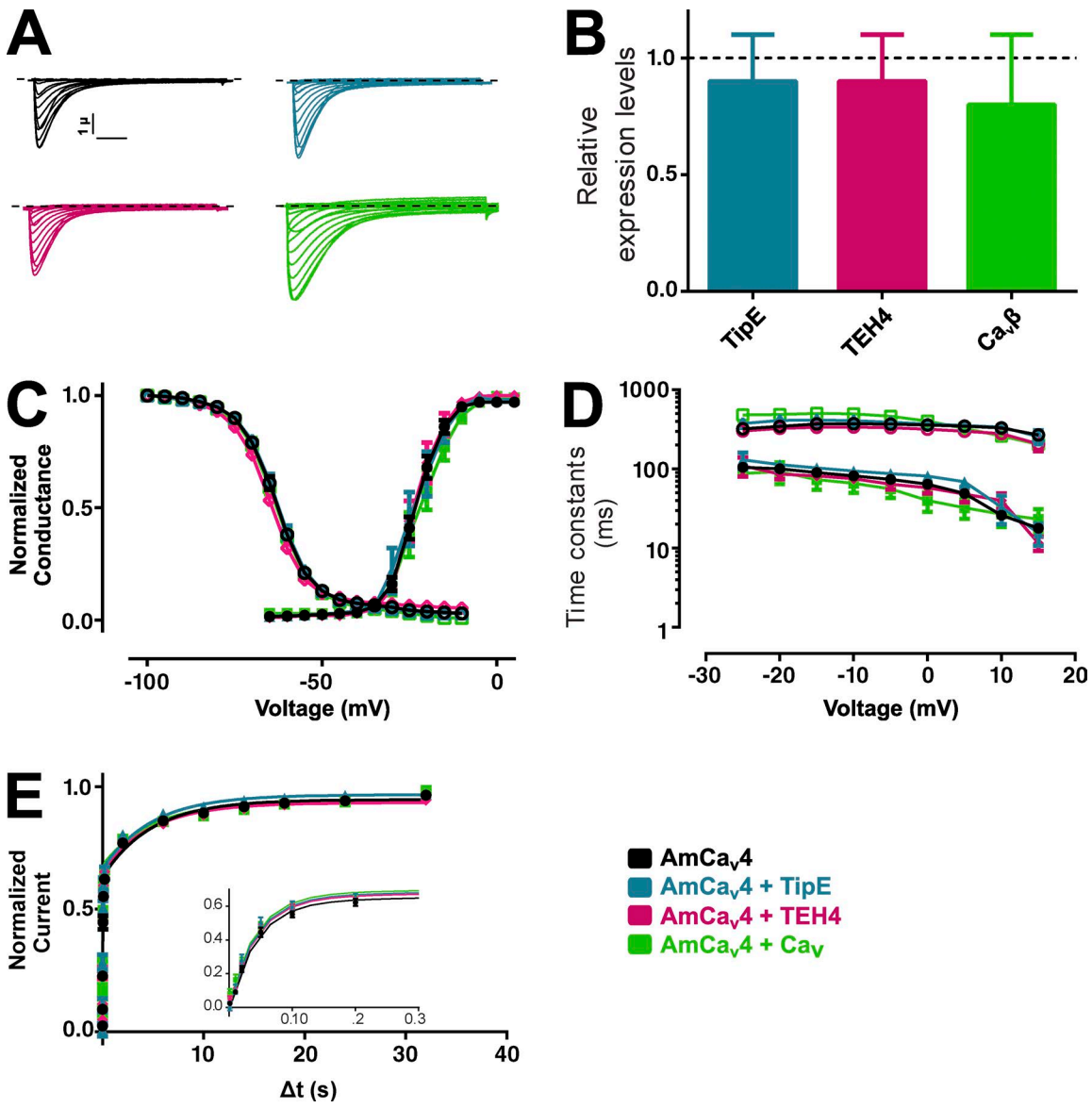


Figure S3. **Effect of known auxiliary subunits on AmCa$_v$4.** (A) Representative current traces recorded in response to the activation protocol with oocytes expressing either AmCa$_v$4 alone or AmCa$_v$4 co-injected with TipE, TEH4, or Ca$_v$βb. (B) Relative expression levels were measured using the same batch of oocytes on the same day and were normalized to the mean maximal conductance recorded for oocytes expressing AmCa$_v$4 alone ($n$ = 7–16). (C) The voltage dependence of activation and inactivation of AmCa$_v$4 was not affected by the coexpression TipE ($n$ = 6–24 for activation, $n$ = 4–12 for inactivation). (D) Time constants measured during the voltage dependence of activation protocol. The time in milliseconds between the start of the stimulation and the peak current recorded for each test pulse is shown in filled symbols. Time constants of current decay are shown in empty symbols. (E) Recovery from inactivation kinetics. Data are expressed as means ± SEM.

Table S1. **Parameters of the Boltzmann equations fitted to the G-V and inactivation curves**

| Parameter | | Mean ± SEM | *n* |
|---|---|---|---|
| **Activation** | | | |
| $V_{1/2}$ (mV) | $AmCa_v4$ | −21.9 ± 1.2 | 24 |
| | $AmCa_v4$ + TipE | −23.3 ± 2.0 | 6 |
| | $AmCa_v4$ + TEH4 | −23.2 ± 1.3 | 6 |
| | $AmCa_v4$ + $Ca_v\beta b$ | −21.5 ± 1.7 | 8 |
| k (mV) | $AmCa_v4$ | −4.5 ± 0.7 | 24 |
| | $AmCa_v4$ + TipE | −3.6 ± 0.5 | 6 |
| | $AmCa_v4$ + TEH4 | −3.5 ± 0.5 | 6 |
| | $AmCa_v4$ + $Ca_v\beta b$ | −4.0 ± 0.4 | 8 |
| **Inactivation** | | | |
| $V_{1/2}$ (mV) | $AmCa_v4$ | −62.3 ± 0.6 | 12 |
| | $AmCa_v4$ + TipE | −62.0 ± 0.7 | 9 |
| | $AmCa_v4$ + TEH4 | −63.9 ± 0.3 | 4 |
| | $AmCa_v4$ + $Ca_v\beta b$ | −62.9 ± 0.8 | 9 |
| k (mV) | $AmCa_v4$ | 6.2 ± 0.2 | 12 |
| | $AmCa_v4$ + TipE | 6.1 ± 0.3 | 9 |
| | $AmCa_v4$ + TEH4 | 6.6 ± 0.2 | 4 |
| | $AmCa_v4$ + $Ca_v\beta b$ | 6.2 ± 0.4 | 9 |

$V_{1/2}$ indicates midpoint and k indicates the slop factor. Data are presented as means ± SEM.

Table S2. **Parameters of the double exponential equations fitted to the recovery from inactivation curves**

| Parameter | | Mean ± SEM | *n* |
|---|---|---|---|
| $A_{fast}$ | $AmCa_v4$ | 0.67 ± 0.02 | 5 |
| | $AmCa_v4$ + TipE | 0.68 ± 0.02 | 6 |
| | $AmCa_v4$ + TEH4 | 0.72 ± 0.01 | 12 |
| | $AmCa_v4$ + $Ca_v\beta b$ | 0.71 ± 0.02 | 5 |
| $\tau_{fast}$ (ms) | $AmCa_v4$ | 50 ± 5 | 5 |
| | $AmCa_v4$ + TipE | 42 ± 3 | 6 |
| | $AmCa_v4$ + TEH4 | 51 ± 4 | 12 |
| | $AmCa_v4$ + $Ca_v\beta b$ | 49 ± 6 | 5 |
| $\tau_{slow}$ (s) | $AmCa_v4$ | 4.7 ± 0.5 | 5 |
| | $AmCa_v4$ + TipE | 4.9 ± 0.9 | 6 |
| | $AmCa_v4$ + TEH4 | 6.4 ± 1.2 | 12 |
| | $AmCa_v4$ + $Ca_v\beta b$ | 8.4 ± 1.8 | 5 |

τ indicates the time constants; A indicates the weight of the time constants. Data are presented as means ± SEM.

Table S3. **Ionic composition of the solutions used to measure the anomalous mole fraction effect**

| Free $Ca^{2+}$ | $Ca(OH)_2$ | EGTA | NaOH | HEPES | NMDG |
|---|---|---|---|---|---|
| | *mM* | *mM* | *mM* | *mM* | *mM* |
| 0 $Ca^{2+}$ | 0 | 10 | 100 | 20 | 10 |
| 20 nM $Ca^{2+}$ | 2 | 9.82 | 100 | 20 | 8.09 |
| 2 µM $Ca^{2+}$ | 2 | 2.08 | 100 | 20 | 11.96 |
| 0.2 mM $Ca^{2+}$ | 0.2 | 0 | 100 | 20 | 14.8 |
| 2 mM $Ca^{2+}$ | 2 | 0 | 100 | 20 | 13 |

## REFERENCE

Gur Barzilai, M., A.M. Reitzel, J.E.M. Kraus, D. Gordon, U. Technau, M. Gurevitz, and Y. Moran. 2012. Convergent evolution of sodium ion selectivity in metazoan neuronal signaling. *Cell Reports.* 2:242–248. http://dx.doi.org/10.1016/j.celrep.2012.06.016